

# Mechanical Actuation of Magnetic Domain-Wall Motion

Se Kwon Kim, Daniel Hill, and Yaroslav Tserkovnyak

*Department of Physics and Astronomy, University of California, Los Angeles, California 90095, USA*

(Dated: May 27, 2019)

We theoretically study the motion of a magnetic domain wall induced by transverse elastic waves in a one-dimensional magnetic wire, which respects both rotational and translational symmetries. By invoking the conservation of the associated total angular and linear momenta, we are able to derive the torque and the force on the domain wall exerted by the waves. We then show how ferromagnetic and antiferromagnetic domain walls can be driven by circularly- and linear-polarized waves, respectively. We envision that elastic waves may provide effective means to drive the dynamics of magnetic solitons in insulators.

PACS numbers: 75.78.-n, 75.60.Ch, 62.30.+d, 63.20.-e

*Introduction.*—Phonons, quanta of elastic vibrations, are ubiquitous in condensed matter systems including magnets. Owing to their gapless nature, they can easily absorb energy from excited spins, thereby engendering the damping term in the description of spin dynamics [1]. Apart from this passive role, the idea of actively using phonons to induce magnetic dynamics has been recently gaining attention in spintronics. For example, it has been experimentally demonstrated that excitation of elastic waves can generate spin currents [2] and thereby drive magnetic bubbles [3].

A domain wall in an easy-axis magnet is one of the simplest and well-studied topological solitons [4], which has practical importance exemplified by the racetrack memory [5]. They can be driven by various means, e.g., a magnetic field [6], a spin-polarized electric current [7], a temperature gradient [8], or a coherent spin wave [9]. Moving domain walls have been known to generate and drag phonons, which in turn gives rise to the damping force on the walls [10]. This force increases as the domain wall approaches the speed of sound, which was pointed out as the origin of the plateau in the dependence of the domain-wall speed on an external field [11].

In this Letter, we study the reciprocal problem: actuation of the magnetic domain-wall motion via the phonon current, which can be injected by mechanical means. Specifically, we consider a one-dimensional magnetic wire with a coaxial easy-axis anisotropy, which can be realized by a single-crystalline iron nanowire embedded in a carbon nanotube [12]. It respects the rotational and translational symmetries and thus conserves the total angular and linear momenta. A magnetic domain wall breaks both symmetries, which opens channels for the exchange of both momenta with phonons. See Fig. 1 for an illustration of a domain-wall configuration for a ferromagnetic system. We show that the domain wall is birefringent for transverse waves and can thus act as a waveplate that alters the circular polarization—and thus the angular momentum—of phonons traveling through it. This change of phonons' angular momentum applies the torque on the domain wall. Reflection of phonons by the

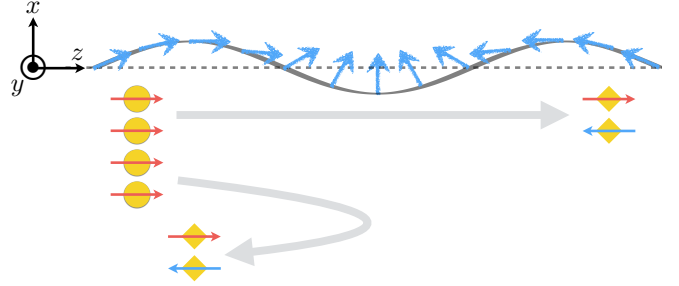


FIG. 1. A schematic illustration of a ferromagnetic wire with a magnetic domain wall (shown by blue thick arrows) and a transverse elastic deformation. The yellow circles represent incoming phonons, quanta of elastic waves; the yellow diamonds represent transmitted and reflected phonons. The red (blue) arrows on circles represent phonons' angular momentum in the positive (negative)  $z$  direction. Phonons are injected from the left; some of them are reflected by the domain wall and thereby exert the force on it; some of the transmitted and reflected phonons change their angular momentum and thereby exert the torque on the wall.

domain wall gives rise to the force acting on it. We study the domain-wall motion induced by the phononic torque and the force in ferromagnets and antiferromagnets.

*Main Results.*—Our model system is a one-dimensional magnetic wire stretched along the global  $z$  axis by an external tension, in which the magnetic order parameter tends to align with the local orientation of the wire. The order parameter is the local spin angular-momentum density for ferromagnets and the local Néel order for antiferromagnets. For temperatures well below the ordering temperature, the local order parameter has the saturated magnitude and thus can be represented by the unit vector  $\mathbf{n}(\zeta, t)$  pointing along its direction. Here,  $\zeta$  is the internal coordinate of the lattice atoms along the wire. In this Letter, we are interested in the interaction between the magnetic soliton—domain wall—and the transverse vibrations of the wire, which are represented by  $u(\zeta, t)$  and  $v(\zeta, t)$  for the displacements of the atom at  $\zeta$  in the lab-frame  $x$  and  $y$  direction, respectively [13]. We shall focus on small displacements by working to the quadratic

order in  $u$  and  $v$ .

The potential energy that involves the magnetic order parameter is given by

$$U_m = \int d\zeta [A\mathbf{n}^{\prime 2} + K\{1 - (\mathbf{n} \cdot \mathbf{t})^2\}], \quad (1)$$

where the positive constants  $A$  and  $K$  are the exchange and anisotropy coefficients, respectively [14]. Here,  $'$  is the derivative with respect to the intrinsic coordinate  $\zeta$ ;  $\mathbf{t}(\zeta, t) \equiv (u', v', \sqrt{1 - u'^2 - v'^2})$  is the unit tangent vector of the wire. The magnetic anisotropy can be rooted in either the magneto-crystalline anisotropy or the shape anisotropy induced by dipolar interactions. When the wire is straight along the  $z$  axis,  $u \equiv v \equiv 0$ , there are two ground states:  $\mathbf{n} \equiv \hat{\mathbf{z}}$  and  $\mathbf{n} \equiv -\hat{\mathbf{z}}$ . A domain wall is a stationary solution of  $\delta_{\mathbf{n}}U_m = 0$  that interpolates two ground states  $\mathbf{n}(\zeta = \pm\infty) = \mp\hat{\mathbf{z}}$  [15]. It is given by [6]

$$n_x(\zeta) = \text{sech}[(\zeta - Z)/\lambda] \cos \Phi, \quad (2a)$$

$$n_y(\zeta) = \text{sech}[(\zeta - Z)/\lambda] \sin \Phi, \quad (2b)$$

$$n_z(\zeta) = -\tanh[(\zeta - Z)/\lambda]. \quad (2c)$$

Here,  $Z$  and  $\Phi$  are the position and the azimuthal angle of the domain wall, respectively;  $\lambda \equiv \sqrt{A/K}$  is the characteristic length scale of the problem, corresponding to the domain-wall width.  $Z$  and  $\Phi$  parametrize two zero modes of the domain wall, which are associated with the breaking of the translational and spin-rotational symmetries. The dynamics of the position  $Z$  induced by the wire's transverse vibrations is of our main interest.

The linearized dynamics of the transverse displacements of the stretched wire can be described by the Lagrangian [16]

$$L_e = \int d\zeta [\mu(\dot{u}^2 + \dot{v}^2) - \mathcal{T}(u'^2 + v'^2)]/2, \quad (3)$$

where the positive constants  $\mu$  and  $\mathcal{T}$  are the mass density of the wire and the applied tension, respectively [17]. The equations of motion for  $u$  and  $v$ , that are derived from the Lagrangian  $L_e$  in conjunction with the potential energy  $U_m$  [Eq. (1)], are given by

$$\mu\ddot{u} - [\{\mathcal{T} + K(n_z^2 - n_x^2)\}u']' = -K(n_z n_x)', \quad (4a)$$

$$\mu\ddot{v} - [\{\mathcal{T} + K(n_z^2 - n_y^2)\}v']' = -K(n_z n_y)'. \quad (4b)$$

For the uniform ground states,  $\mathbf{n} \equiv \pm\hat{\mathbf{z}}$ , the right-hand sides vanish and the tension is effectively increased from  $\mathcal{T}$  to  $\mathcal{T}_\kappa \equiv (1 + \kappa)\mathcal{T}$  with  $\kappa \equiv K/\mathcal{T}$ . The dispersion relation is then given by  $\omega = \pm v_0 k$  with the speed  $v_0 \equiv \sqrt{\mathcal{T}_\kappa/\mu}$ . Using the propagating-wave solutions to the above equations in the presence of the domain wall, details of which will be shown later, we can derive the torque and the force on the wall by the phonon current.

The magnetic domain wall breaks the rotational and translational symmetries by selecting an azimuthal angle

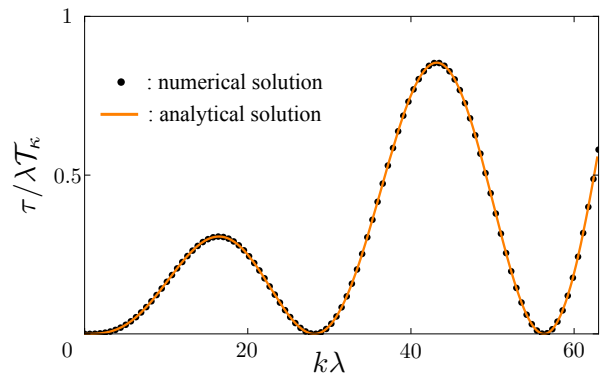


FIG. 2. The torque  $\tau$  on the domain wall by the circularly-polarized waves as a function of the wavenumber  $k\lambda$  for the parameters  $\kappa = 0.2$  and  $a = \lambda/10$ . The solid line is obtained with the analytical expression for  $\tau$  in Eq. (5); the dots are obtained with  $\tau$  in Eq. (13) calculated from numerical solutions of the differential equations (7).

$\Phi$  and a position  $Z$ , respectively. Incoming elastic waves thereby scatter off the domain wall. By invoking the conservation of both momenta, we are able to derive the torque  $\tau$  and the force  $F$  on the domain wall. Let us present main features in the case of a small anisotropy  $\kappa \ll 1$ , which allows us to neglect the backaction of the induced domain-wall motion on the elastic waves in Eqs. (4).

First, circularly-polarized waves incoming from the left,  $u(\zeta, t) = a \cos(k\zeta - \omega t)$  and  $v(\zeta, t) = -a \sin(k\zeta - \omega t)$ , exert the torque (i.e., the transfer of angular momentum) on the domain wall,

$$\tau \simeq \mathcal{T}_\kappa a^2 k [1 - \cos\{k\lambda \ln(1 - \kappa)\}], \quad (5)$$

for high-energy waves  $k\lambda \gg 1$  [18], which is obtained by the subtraction of the angular momentum current of the transmitted wave,  $\mathcal{T}_\kappa a^2 k \cos\{k\lambda \ln(1 - \kappa)\}$ , from that of the incoming wave,  $\mathcal{T}_\kappa a^2 k$ . The physical origin of the torque can be understood as follows. From Eqs. (4), the domain wall locally modifies the tension for the  $u$  and  $v$  displacements by  $K[1 - 2\text{sech}^2(\zeta/\lambda)]$  and  $K[1 - \text{sech}^2(\zeta/\lambda)]$ , respectively. The  $v$  component thus propagates faster than the  $u$  component within the domain wall, which acts as a birefringent medium that can alter the polarization of the wave. The argument of the cosine function in Eq. (5) is the relative phase shift of  $u$  and  $v$  components of the transmitted wave,  $\phi_{u,t} - \phi_{v,t} \simeq k\lambda \ln(1 - \kappa)$ . For example, when the relative phase shift is  $\pi \pmod{2\pi}$ , the transmitted wave carries the angular momentum polarized in the opposite direction of the incoming wave, and thus the efficiency of angular-momentum transfer from the wave to the domain wall attains its maximum. Figure 2 shows the torque  $\tau$  as a function of the wavenumber  $k\lambda$ . Note that it oscillates as a function of  $k\lambda$  with the period of  $2\pi/\ln(1 - \kappa)$ . This torque by the elastic waves can drive ferromagnetic

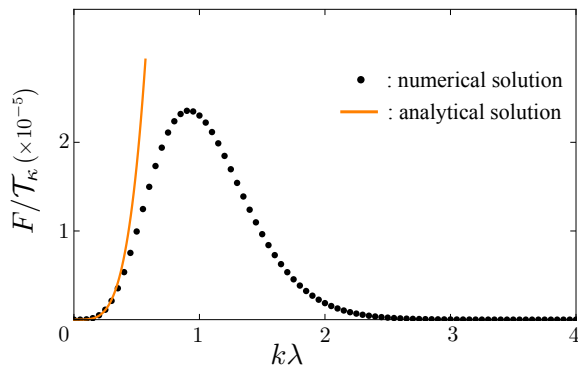


FIG. 3. The force  $F$  on the domain wall exerted by the linearly-polarized waves perpendicular to the wall plane for the parameters  $\kappa = 0.2$  and  $a = \lambda/10$ . The solid line is obtained with the analytical expression for  $F$  in Eq. (6); the dots are obtained with  $F$  in Eq. (14) calculated from numerical solutions of the differential equations (7).

domain walls, analogous to the torque of spin waves [9]. The steady-state speed of the ferromagnetic domain wall is  $V = \tau/2s$  [Eq. (17)] in the absence of damping, where  $s \equiv \hbar S/\mathcal{V}$  is the saturated spin density ( $\mathcal{V}$  is the volume per spin).

Secondly, linearly-polarized waves incoming from the left,  $v(\zeta, t) = a \cos(k\zeta - \omega t)$  and  $u(\zeta, t) \equiv 0$ , exert no torque, yet there is a finite force (i.e., the transfer of linear momentum) on the domain wall due to the reflection,

$$F \simeq \mathcal{T}_\kappa \kappa^2 \lambda^2 a^2 k^4, \quad (6)$$

for low-energy waves  $k\lambda \ll 1$ . It is the product of the pressure (i.e., the linear momentum current) of the incoming wave,  $\mathcal{T}_\kappa a^2 k^2/2$ , and twice the reflection probability,  $2\kappa^2 \lambda^2 k^2$  [19]. The reflection probability is exponentially small for high-energy waves  $k\lambda \gg 1$ , and so is the force. Figure 3 shows the force  $F$  as a function of the wavenumber  $k\lambda$ . This force of the elastic waves can drive antiferromagnetic domain walls, analogous to the force of spin waves [9, 20]. The steady-state speed of the antiferromagnetic domain wall is  $V = \lambda F/2\alpha s$  [Eq. (18)], where  $\alpha$  is the Gilbert damping constant.

*Transverse waves.*—Let us solve the differential equations (4) for  $u$  and  $v$  in the presence of the static domain wall given by Eqs. (2). A general solution is composed of static and dynamic components. A static one is determined by the right-hand sides of the equations [21], whereas dynamic components, which are of interest to us, are the propagating waves, for which we can neglect the right-hand sides. For the monochromatic solutions, i.e.,  $\propto \exp(-i\omega t)$ , the equations are given by

$$[\{1 - 2\tilde{\kappa} \operatorname{sech}^2(\zeta/\lambda)\} u']' = -k^2 u, \quad (7a)$$

$$[\{1 - \tilde{\kappa} \operatorname{sech}^2(\zeta/\lambda)\} v']' = -k^2 v, \quad (7b)$$

with  $k^2 \equiv \omega^2/v_0^2$  and  $\tilde{\kappa} \equiv \kappa/(1 + \kappa)$ . We shall focus

on solutions for  $v$  henceforth, from which we can obtain solutions for  $u$  by replacing  $\tilde{\kappa}$  by  $2\tilde{\kappa}$ . For the given incoming-wave component, the solution far away from the wall can be characterized by four real numbers: the amplitude  $t > 0$  and the phase-shift  $\phi_t$  of the transmitted component and the amplitude  $r > 0$  and the phase-shift  $\phi_r$  of the reflected component:

$$v(\zeta) \propto \begin{cases} e^{ik\zeta} + r e^{-ik\zeta + i\phi_r}, & \text{for } \zeta \ll -\lambda \\ t e^{ik\zeta + i\phi_t}, & \text{for } \zeta \gg \lambda. \end{cases} \quad (8)$$

The equation can be transformed into a quantum-mechanic scattering problem by introducing a new coordinate  $\eta$  satisfying  $d\zeta/d\eta = 1 - \tilde{\kappa} \operatorname{sech}^2(\zeta/\lambda)$  [22]:

$$\left[ -\frac{d^2}{d\eta^2} + k^2 \tilde{\kappa} \operatorname{sech}^2 \frac{\zeta(\eta)}{\lambda} \right] v = k^2 v. \quad (9)$$

We then need to find a solution for the wavefunction  $v$  with the energy  $k^2$  in the presence of the localized potential  $k^2 \tilde{\kappa} \operatorname{sech}^2[\zeta(\eta)/\lambda]$ .

The exact analytical solutions are not available. Instead, we obtain approximate solutions in the two extreme energy regimes. First, in the high-energy limit,  $k\lambda \gg 1$ , we can use the Wentzel-Kramers-Brillouin (WKB) approximation [23]. The solution in the first-order real-space WKB approximation is  $v(\zeta) \propto \exp[ik \int d\zeta \{1 - \tilde{\kappa} \operatorname{sech}^2(\zeta/\lambda)\}^{-1/2}]$  in the original coordinate  $\zeta$  with the transmission amplitude  $t = 1$ . The phase shift of the transmitted wave is given by

$$\phi_t = k \int_{-\infty}^{\infty} \frac{d\zeta}{\sqrt{1 - \tilde{\kappa} \operatorname{sech}^2(\zeta/\lambda)}} = -k\lambda \ln(1 - \tilde{\kappa}). \quad (10)$$

In the low-energy limit, we approximate the potential by the delta-function barrier with the height  $h_k \equiv 2k^2 \sqrt{\tilde{\kappa}/(1 - \tilde{\kappa})} \arcsin \sqrt{\tilde{\kappa}}$  that is the integral of the potential from  $\eta = -\infty$  to  $\eta = \infty$ . After solving the scattering problem with the delta-function potential and going back to the original coordinate  $\zeta$ , we obtain

$$r = \tilde{\kappa} k \lambda, \quad \phi_r = -\pi/2, \quad t = 1, \quad \phi_t = \tilde{\kappa} k \lambda, \quad (11)$$

to the first order in  $k\lambda$ . Note that for a small anisotropy,  $\tilde{\kappa} \ll 1$ , the phase shifts of the transmitted wave in the two regimes coincide:  $-k\lambda \ln(1 - \tilde{\kappa}) \simeq \tilde{\kappa} k \lambda$ .

*Torque and force.*—In the uniform magnetic state,  $\mathbf{n}(\zeta) \equiv \hat{\mathbf{z}}$ , the effective Lagrangian density for the waves which includes the effect of the anisotropy is given by  $\mathcal{L} = \mu(\dot{u}^2 + \dot{v}^2) - \mathcal{T}_\kappa(u^2 + v^2)$ . Axial symmetry of the Lagrangian implies conservation of the corresponding angular momentum. The temporal and spatial components of the associated Nöther current [20, 24] are given by  $\rho^s = \mu(u\dot{v} - v\dot{u})$  and  $I^s = -\mathcal{T}_\kappa(uv' - v'u')$ , which are, respectively, the density and the current of the (orbital) angular momentum. We can also obtain the linear momentum density  $T^{10} = -\mu\dot{u}u' + (u \rightarrow v)$  and the current

$T^{11} = (\mu\dot{u}^2 + \mathcal{T}_\kappa u^2)/2 + (u \rightarrow v)$  from the stress-energy tensor,  $T^{\alpha\beta} \equiv \partial^\alpha u [\partial \mathcal{L} / \partial (\partial_\beta u)] + (u \rightarrow v) - \delta^{\alpha\beta} \mathcal{L}$  [24]. For monochromatic waves,  $u(\zeta, t) = u_0 \cos(k\zeta - \omega t)$  and  $v(\zeta, t) = v_0 \cos(k\zeta - \omega t + \Delta\phi)$ , the angular and linear momentum currents are respectively given by

$$I^s = \mathcal{T}_\kappa u_0 v_0 \sin(\Delta\phi)k, \quad T^{11} = \mathcal{T}_\kappa (u_0^2 + v_0^2)k^2/2, \quad (12)$$

where we used the dispersion relation  $\omega^2 = v_0^2 k^2$ .

An intuitive way to understand these momentum currents is to picture the elastic wave as a flux of phonons, particles carrying the angular momentum  $\pm\hbar$  and the linear momentum  $\hbar k$ . Let us take an example of a circularly-polarized wave with  $u_0 = v_0 = a$  and  $\Delta\phi = \pi/2$ , which has the angular and the linear momentum current,  $I^s = \mathcal{T}_\kappa a^2 k$  and  $T^{11} = \mathcal{T}_\kappa a^2 k^2$ . We can obtain the number current from the linear momentum current by  $T^{11}/\hbar k = \mathcal{T}_\kappa a^2 k/\hbar$ . Comparison between the number current and the angular momentum current leads us to conclude that phonons in the wave has the angular momentum  $+\hbar$  (polarized along the  $\hat{z}$  axis).

Let us now derive the torque and the force on the domain wall exerted by elastic waves incoming from the left,  $\zeta = -\infty$ . The torque is the difference of the angular momentum current  $I^s$  between the far left and far right of the domain wall; the force is the difference of the linear momentum current  $T^{11}$  between them. First, for the circularly-polarized incoming wave,  $u(\zeta, t) = a \cos(k\zeta - \omega t)$  and  $v(\zeta, t) = -a \sin(k\zeta - \omega t)$ , the time-averaged torque and force are given by

$$\tau = \mathcal{T}_\kappa a^2 (1 - t_u t_v \cos \Delta\phi_t - r_u r_v \cos \Delta\phi_r)k, \quad (13)$$

$$F = \mathcal{T}_\kappa a^2 (r_u^2 + r_v^2)k^2, \quad (14)$$

where  $t_u$  and  $t_v$  are respectively the transmission amplitudes of the  $u$  and  $v$  components (and similarly  $r_u$  and  $r_v$  for the reflection amplitudes) and  $\Delta\phi_t$  is the relative phase shift of the transmitted  $u$  and  $v$  components (and similarly  $\Delta\phi_r$  for the reflected wave). Equation (5) for  $\tau$  is the reflectionless limit of Eq. (13), corresponding to  $k\lambda \gg 1$ . Secondly, for the linearly-polarized incoming wave,  $v(\zeta, t) = a \cos(k\zeta - \omega t)$ , the torque vanishes and the force is given by

$$F = \mathcal{T}_\kappa a^2 r_v^2 k^2. \quad (15)$$

*Ferromagnetic domain wall.*—The dynamics of the ferromagnet is described by the Lagrangian [25],  $L = s \int d\zeta \mathbf{a}(\mathbf{n}) \cdot \mathbf{n} - U[\mathbf{n}]$ , where  $\mathbf{a}(\mathbf{n})$  is a vector potential of a magnetic monopole,  $\nabla_{\mathbf{n}} \times \mathbf{a} = \mathbf{n}$ . The angular and linear momenta of the head-to-head domain wall [Eqs. (2)] in ferromagnets are given by, respectively,  $J = J_0 + 2sZ$  and  $P = P_0 - 2s\Phi$ , where  $J_0$  and  $P_0$  are arbitrary real numbers that can be interpreted as gauge choices [26, 27]. In the Lagrangian formalism, viscous losses are represented by the Rayleigh dissipation function [24]  $R = \alpha s \int d\zeta \dot{\mathbf{n}}^2/2$ , where  $\alpha$  is Gilbert's damping

constant [1]. By plugging the domain-wall solution, we obtain  $R = \alpha s (\lambda \dot{\Phi}^2 + \dot{X}^2/\lambda)$ . The conservations of the total angular and linear momenta yield their equations of motion,

$$\tau = \dot{J} + 2\alpha s \lambda \dot{\Phi}, \quad F = \dot{P} + 2\alpha s \dot{Z}/\lambda. \quad (16)$$

The steady-state velocity  $V = \dot{Z}$  is given by

$$V = \frac{\tau + \alpha \lambda F}{2(1 + \alpha^2)s}. \quad (17)$$

*Antiferromagnetic domain wall.*—The dynamics of the antiferromagnet is described by the Lagrangian,  $L = \rho \int d\zeta \dot{\mathbf{n}}^2/2 - U[\mathbf{n}]$ , where  $\rho$  quantifies inertia of the order parameter [28]. The Rayleigh dissipation function is  $R = \alpha s \int d\zeta \dot{\mathbf{n}}^2/2$  [29]. For slow dynamics, the angular and linear momenta of the domain wall are respectively given by  $J = I\dot{\Phi}$  and  $P = M\dot{Z}$ , where  $I \equiv 2\rho\lambda$  and  $M \equiv 2\rho/\lambda$  are the moment of inertia and the mass of a static domain wall [20]. Their equations of motion are same as Eqs. (16). The steady-state velocity  $\dot{Z}(t) \rightarrow V$  is given by

$$V = \frac{\lambda F}{2\alpha s}. \quad (18)$$

*Discussion.*—We have studied the effects of transverse waves on the domain-wall motion while neglecting other types of waves such as longitudinal or torsional ones [30] by focusing on systems, where their energy scales are well separated so that we can study them separately. The other waves, however, also can exert the torque and the force on the domain wall.

By flipping the sign of  $K$  in the potential energy  $U_m$  [Eq. (1)], we can describe easy-plane magnets, which support superfluid spin transport [31]. The interaction between elastic deformations and spin superfluidity can be studied by invoking the conservation of the total angular and linear momenta as done in this Letter.

Reversing the roles of elasticity and magnetism provides another interesting problem. At temperatures lower than the spin-Peierls transition temperature, a one-dimensional spin lattice is dimerized [32], which can occur in two different ways. An equilibrium lattice configuration interpolating the two dimerization patterns is referred to as an elastic soliton [33]. Investigating how to drive the elastic soliton with spin waves may serve as a future research topic.

We are grateful for discussions with Héctor Ochoa and Ricardo Zarzuela, who helped us to formulate the problem. This work was supported by the Army Research Office under Contract No. 911NF-14-1-0016 and, in part, by FAME (an SRC STARnet center sponsored by MARCO and DARPA).

---

[1] T. Gilbert, IEEE Trans. Magn. **40**, 3443 (2004).

- [2] K. Uchida, H. Adachi, T. An, T. Ota, M. Toda, B. Hillebrands, S. Maekawa, and E. Saitoh, *Nat. Mater.* **10**, 737 (2011); M. Weiler, H. Huebl, F. S. Goerg, F. D. Czeschka, R. Gross, and S. T. B. Goennenwein, *Phys. Rev. Lett.* **108**, 176601 (2012).
- [3] N. Ogawa, W. Koshibae, A. J. Beekman, N. Nagaosa, M. Kubota, M. Kawasaki, and Y. Tokura, *Proc. Natl. Acad. Sci.* **112**, 8977 (2015).
- [4] A. Kosevich, B. Ivanov, and A. Kovalev, *Phys. Rep.* **194**, 117 (1990), and references therein.
- [5] S. S. P. Parkin, M. Hayashi, and L. Thomas, *Science* **320**, 190 (2008).
- [6] N. L. Schryer and L. R. Walker, *J. Appl. Phys.* **45**, 5406 (1974).
- [7] J. Slonczewski, *J. Magn. Magn. Mater.* **159**, L1 (1996); L. Berger, *Phys. Rev. B* **54**, 9353 (1996); A. C. Swaving and R. A. Duine, *Phys. Rev. B* **83**, 054428 (2011); K. M. D. Hals, Y. Tserkovnyak, and A. Brataas, *Phys. Rev. Lett.* **106**, 107206 (2011).
- [8] A. A. Kovalev and Y. Tserkovnyak, *Europhys. Lett.* **97**, 67002 (2012); W. Jiang, P. Upadhyaya, Y. Fan, J. Zhao, M. Wang, L.-T. Chang, M. Lang, K. L. Wong, M. Lewis, Y.-T. Lin, J. Tang, S. Cherepov, X. Zhou, Y. Tserkovnyak, R. N. Schwartz, and K. L. Wang, *Phys. Rev. Lett.* **110**, 177202 (2013).
- [9] P. Yan, X. S. Wang, and X. R. Wang, *Phys. Rev. Lett.* **107**, 177207 (2011); E. G. Tveten, A. Qaiumzadeh, and A. Brataas, *Phys. Rev. Lett.* **112**, 147204 (2014).
- [10] V. G. Bar'yakhtar, B. A. Ivanov, and M. V. Chetkin, *Sov. Phys. Usp.* **28**, 563 (1985), and references therein.
- [11] S. O. Demokritov, A. I. Kirilyuk, N. M. Kreines, V. I. Kudinov, V. B. Smirnov, and M. V. Chetkin, *J. Magn. Magn. Mater.* **102**, 339 (1991).
- [12] K. Lipert, S. Bahr, F. Wolny, P. Atkinson, U. Weißker, T. Mühl, O. G. Schmidt, B. Büchner, and R. Klingeler, *App. Phys. Lett.* **97**, 212503 (2010).
- [13] By assuming that the Young's modulus is much larger than the applied tension,  $E \gg \mathcal{T}$ , we shall neglect longitudinal displacements by focusing on low-energy transverse modes [16, 24, 34].
- [14] Transverse elastic deformations may affect the magnetic potential energy by modifying the geometry of the wire, which can be captured by an additional potential-energy term  $\delta U_m = \int d\zeta (u'^2 + v'^2) [\xi \mathbf{A} \mathbf{n}'^2 + \nu K \{1 - (\mathbf{n} \cdot \mathbf{t})^2\}] / 2$ , where  $\xi$  and  $\nu$  are the dimensionless parameters that account for effects of geometrical deformations on the exchange and anisotropy energies, respectively. This term modifies the strength of the potential (induced by a magnetic domain wall) for elastic waves in Eq. (7),  $2\tilde{\kappa} \mapsto [2 - (\xi + \nu)]\tilde{\kappa}$  for  $u$  and  $\tilde{\kappa} \mapsto [1 - (\xi + \nu)]\tilde{\kappa}$  for  $v$ , which does not change the elastic-wave-induced motion of the domain wall qualitatively. In particular, the term does not distinguish two transverse modes,  $u$  and  $v$ , and thus does not destroy the birefringence of the domain wall with respect to them, which causes the torque on the wall in Eq. (5).
- [15] There are two types of domain walls depending on the boundary conditions: a head-to-head domain wall for  $\mathbf{n}(\zeta = \pm\infty) = \mp \hat{\mathbf{z}}$  (assumed here) and a tail-to-tail domain wall for  $\mathbf{n}(\zeta = \pm\infty) = \pm \hat{\mathbf{z}}$ .
- [16] M. Kardar, *Statistical Physics of Fields* (Cambridge University Press, Cambridge, 2007).
- [17] The elastic energy of the wire also contains the bending energy  $\propto (u'')^2$  [35], but we neglect it by assuming the long-wavelength limit, in which the tension is strong enough so that the potential energy  $\propto T$  in  $L_e$  dominates over the bending energy.
- [18] The force on the wall is exponentially small for high-energy waves, which is why we decided to focus on the torque here.
- [19] In terms of phonons, it is the product of the incoming phonon number current,  $\mathcal{T}_\kappa a^2 k / 2\hbar$ , the change of the reflected phonon's linear momentum,  $2\hbar k$ , and the reflection probability.
- [20] S. K. Kim, Y. Tserkovnyak, and O. Tchernyshyov, *Phys. Rev. B* **90**, 104406 (2014).
- [21] The theoretical studies on the interaction of the fast-moving domain walls with the lattice deformations focused on the static solutions. See Refs. [10] and [36].
- [22] The close expression for  $\eta$  in terms of  $\zeta$  is  $\eta = \zeta + \sqrt{\tilde{\kappa}/(1 - \tilde{\kappa})} \arctan[\sqrt{\tilde{\kappa}/(1 - \tilde{\kappa})} \tanh \zeta]$  up to an arbitrary constant.
- [23] L. D. Landau and E. M. Lifshitz, *Quantum Mechanics*, 3rd ed. (Butterworth-Heinemann, Oxford, 1976).
- [24] H. Goldstein, C. Poole, and J. Safko, *Classical Mechanics*, 3rd ed. (Addison Wesley, 2002).
- [25] A. Altland and B. Simons, *Condensed Matter Field Theory* (Cambridge University Press, Cambridge, 2006).
- [26] P. Yan, A. Kamra, Y. Cao, and G. E. W. Bauer, *Phys. Rev. B* **88**, 144413 (2013).
- [27] O. Tchernyshyov, *Ann. Phys.* **363**, 98 (2015).
- [28] I. V. Bar'yakhtar and B. A. Ivanov, *Fiz. Nizk. Temp.* **5**, 759 (1979); A. F. Andreev and V. I. Marchenko, *Sov. Phys. Usp.* **23**, 21 (1980).
- [29] H. V. Gomonay and V. M. Loktev, *Phys. Rev. B* **81**, 144427 (2010).
- [30] L. Landau and E. Lifshitz, *Theory of Elasticity*, 3rd ed. (Butterworth-Heinemann, Oxford, 1986).
- [31] E. B. Sonin, *Adv. Phys.* **59**, 181 (2010), and references therein.
- [32] E. Pytte, *Phys. Rev. B* **10**, 4637 (1974).
- [33] T. Nakano and H. Fukuyama, *J. Phys. Soc. Jpn.* **49**, 1679 (1980).
- [34] E. I. Butikov, *Phys. Scr.* **86**, 035403 (2012).
- [35] P. M. Chaikin and T. C. Lubensky, *Principles of Condensed Matter Physics* (Cambridge University Press, Cambridge, 2000).
- [36] A. K. Zvezdin and A. A. Mukhin, *Sov. Phys. JETP* **75**, 306 (1992).